

HIGH PRECISION CAVITY SIMULATIONS*

W. Ackermann**, T. Weiland, Technische Universität Darmstadt,
 Institut für Theorie Elektromagnetischer Felder (TEMF),
 Schlossgartenstraße 8, 64289 Darmstadt, Germany

Abstract

The design of resonant radio frequency cavities used in particle accelerator machines to accelerate charged particles of various species is heavily based on proper computer simulations. While the determination of the resulting field distribution can be obtained by analytical means only for a limited number of cavity shapes it is essential to apply appropriate computer programs to find sufficiently accurate approximate solutions. The achievable quality first depends on the underlying mathematical model which then has to be solved accurately on a discrete level. The precise knowledge of the distribution of the electromagnetic fields both within the cavities as well as on the surface of the resonators is essential for appropriate cavity-shape optimizations and accurate beam dynamics studies.

INTRODUCTION

In the context of highly resonating cavities a promising method to determine the electromagnetic field distribution inside the structures is given by the eigenmode analysis where a limited number of eigensolutions is used to characterize the devices within a specified frequency range. Selected eigenmodes can be determined with the help of suitable eigenmode solvers once the underlying continuous mathematical model is properly transformed into a convenient matrix formulation. Under actual operating conditions, the fields in the resonators have to be coupled to the fields in the external devices either to enable energy transfer from e.g. the sources to the beam or, conversely, to dump beam-driven parasitic modes to internal or external loads. Compared to lossless standing-wave structures where real-valued variables are sufficient to describe the entire field distribution this is no longer true in a dissipative environment where a resulting net energy transfer has to be supported. On the other hand, a complex-valued formulation completely enables to describe the physical space-dependent phase variation and additionally allows to characterize the oscillation by simultaneously extracting the corresponding quality factor next to the resonance frequency. Unfortunately, the solution of complex-valued eigenvalue systems is much more demanding compared to the widespread real-valued formulations and special care has to be put in the implementation of the computer programs to achieve good performances for large-scale applications.

* Work partially supported by DESY, Hamburg

**ackermann@temf.tu-darmstadt.de

MATHEMATICAL MODELING

A proper mathematical model to describe the electromagnetic field distribution within highly resonating structures with an eigenmode analysis in mind is obviously based on Maxwell's equations in frequency domain. We use the differential notation

$$\text{curl } \vec{H} = \vec{J} + j\omega\vec{D} \quad (1a)$$

$$\text{curl } \vec{E} = -j\omega\vec{B} \quad (1b)$$

$$\text{div } \vec{B} = 0 \quad (1c)$$

$$\text{div } \vec{D} = \rho \quad (1d)$$

to point out the interdependence of the applied electromagnetic field components. In this context, \vec{E} and \vec{H} represent the phasors of the electric and magnetic field strength while \vec{D} and \vec{B} specify the electric and magnetic flux densities, respectively. The symbol ω represents the angular frequency while \vec{J} and ρ describe the sources of the electromagnetic fields. In the following we concentrate on linear isotropic materials which may be inhomogeneous if required. This limitation simplifies the material relations to $\vec{D} = \epsilon\vec{E}$ and $\vec{B} = \mu\vec{H}$ with space-depending scalar proportionality factors. Finally, the electric conductivity σ give rise to the electric current density $\vec{J} = \sigma\vec{E}$ which is responsible for the specific bulk-related losses.

Discretization

To transform the continuous formulation into a suitable matrix equation we discretize (1) with the help of the finite element method (FEM) [1]. Eliminating either the electric or the magnetic field combines the two first-order differential equations into one second-order equation. This procedure simplifies the overall solution process because only one type of field either with tangential or normal continuity conditions has to be properly represented on the discrete level. In the end, the initially eliminated field can be reconstructed in a postprocessing step if one of the curl relations in (1) is applied to the selected quantity.

With the well-known Nédélec elements in mind we set the focus of the formulation on the electric field only and combine (1a) and (1b) to the double-curl equation

$$\text{curl} \left(\frac{1}{\mu} \text{curl } \vec{E} \right) + j\omega\vec{J} - \omega^2\epsilon\vec{E} = 0 \quad (2)$$

which finally will be discretized following Galerkin's approach. The electric field strength $\vec{E} = \sum_i x_i \vec{\omega}_i^{3D}$ is expanded in terms of locally defined real-valued vector basis

functions such that the introduced degrees of freedom x_i have to be of complex type [2].

Collecting the unknown weighting coefficients x_i in the vector variable \vec{x} allows to formulate the entire problem in terms of the eigenvalue problem

$$A^{3D}\vec{x} + j\omega\mu_0 C^{3D}\vec{x} - \omega^2\mu_0\varepsilon_0 B^{3D}\vec{x} = 0 \quad (3)$$

which has to be solved accurately to fulfill the full set of Maxwell's equations also on the discrete level. This is especially important because the fundamental charge relation (1d) is not explicitly stated in the problem formulation but will be implicitly satisfied in the dynamic case once the curl equations are properly treated. The matrices A^{3D} , B^{3D} and C^{3D} in (3) are specified according to their components

$$A_{ij}^{3D} = \iiint_{\Omega} \frac{1}{\mu_r} \text{curl } \vec{\omega}_i^{3D} \cdot \text{curl } \vec{\omega}_j^{3D} d\Omega \quad (4a)$$

$$B_{ij}^{3D} = \iiint_{\Omega} \varepsilon_r \vec{\omega}_i^{3D} \cdot \vec{\omega}_j^{3D} d\Omega \quad (4b)$$

$$C_{ij}^{3D} = \iiint_{\Omega} \sigma \vec{\omega}_i^{3D} \cdot \vec{\omega}_j^{3D} d\Omega \quad (4c)$$

and are sparsely populated on principle because of the local support of the applied basis functions.

If losses are considered in the simulation the resulting damping behavior of the oscillation is naturally described by an occurring imaginary part of the angular frequency. Conversely, if neither conductive material is available within the computational domain nor any boundary-related loss mechanism has to be considered the matrix system (3) reduces to a classical generalized eigenvalue problem which can be solved following standard techniques.

Boundary Conditions

The important boundary conditions are incorporated into the system with the help of the surface contribution

$$-j\omega\mu_0 \iint_A (\vec{n} \times \vec{H}) \cdot \vec{\omega}_j^{3D} dA \quad (5)$$

which originates from a partial integration of the fundamental double-curl contribution in combination with Faraday's law (1b) to eliminate the emerging curl of the electric field strength. There is a large variety of possible boundary conditions available to encapsulate the computational domain from the remaining structure. Regarding cavity simulations the most important and often idealized boundary conditions are specified as follows:

- Perfect magnetic conductive material (PMC):

The interface condition to perfect magnetic conductive material is characterized by vanishing tangential magnetic field components in the interface plane. With \vec{n} representing the local surface normal vector an appropriate relation is given by $\vec{n} \times \vec{H} = 0$ which prevents the boundary integral (5) to contribute to the overall FEM formulation and is therefore known as

the natural boundary condition of the method. In the context of eigenmode analysis the magnetic boundary condition is used to realize symmetry planes.

- Perfect electric conductive material (PEC):

The interface condition to perfect electric conductive material is characterized by vanishing tangential electric field components in the interface plane. This widespread boundary condition is not represented with the help of the boundary integral (5) but will be incorporated into the final formulation by explicitly forcing the corresponding weighting coefficients of the applied Nédélec-type vector basis functions to be zero. The integral (5) finally does not contribute to the formulation because the adjacent vector basis functions do not show any tangential component to the surface. An efficient implementation will eliminate those contributions a priori and therefore has to distinguish between volume and surface related basis functions. The electric boundary condition is applied to realize symmetry planes and to approximate the metallic surfaces of superconducting cavities.

- Impedance boundary condition:

One of the local acting lossy boundary conditions which can be used to formulate the necessary energy exchange in the interface plane is given by the impedance relation $Z(\vec{n} \times \vec{H}) = \vec{n} \times (\vec{n} \times \vec{E})$ where Z represents the ratio of the tangential electric to the magnetic field strength. Incorporating this representation into the boundary formulation (5) results in

$$j\omega\mu_0 \iint_A \frac{1}{Z} (\vec{n} \times \vec{\omega}_i^{3D}) \cdot (\vec{n} \times \vec{\omega}_j^{3D}) dA \quad (6)$$

while the integral part can be immediately added to the system matrix (4c) if the specified impedance is modeled independent of the frequency. If a frequency dependent representation has to be resolved in the system (3) the matrix equation turns from quadratic to higher-order polynomial or even nonlinear in general and radically increases the requirements on the underlying eigenvalue solver. With respect to the cavity eigenmode calculation the concept of impedance boundary condition leads to the most simple approach to enable wave propagation in either coaxial lines attached to the resonators with the help of carefully designed coupler units or the beam tubes. Unfortunately, this efficient formulation is restricted to single-mode propagation only so that the usable frequency range is limited to the interval of fundamental mode transport in the particular waveguides. Compared to more generally applicable boundary conditions the formulation in (6) advantageously retains the sparsity pattern of the original system and does not introduce additional matrix elements. This favorable property is of particular importance if efficient eigenvalue solvers have to be implemented where preconditioners are applied to solve linear systems of equations.

- Port boundary condition:

Accelerating cavities are necessarily equipped with fundamental couplers to enable the energy transfer from the radio-frequency sources to the beam. In the same way intentionally installed highly-specialized couplers allow the extraction of parasitic modes to prevent performance degradation in high-current applications. While a single-mode wave propagation can be efficiently modeled with the help of the impedance boundary condition this is no longer true for the multi-mode case. The accurate modeling of a true port interface can be realized with the help of a two-dimensional (2-D) modal expansion of the resulting electromagnetic field in the specified boundary plane. This procedure enables the correct treatment of any kind of wave propagation in the attached line including even the excitation below cut-off. This ability is especially interesting even for the simple mono-mode case because the port-interface plane can then be located near to the cavity where higher-order modes still have to be considered. Following this approach a large amount of degrees of freedom can be saved because otherwise the interface plane has to be moved far away from the cavity to guarantee that all higher-order modes are sufficiently decayed. The modeling of the coaxial lines is particularly expensive because it naturally requires a fine grid resolution to resolve the small geometric details. The numerical treatment of the port boundary condition is established again with the help of the boundary integral representation (5) in combination with Faraday's law (1b) because the presented three-dimensional (3-D) formulation is based on the electric field strength only. A full modal approach has to consider all modes traveling in both directions of the attached waveguide

$$\vec{E} = \sum_{\nu} \left(A_{\nu}^{(-)} \vec{E}_{\nu}^{(-)} + A_{\nu}^{(+)} \vec{E}_{\nu}^{(+)} \right) \quad (7)$$

with the incoming waves representing the desired excitation. Keeping the aspired eigenvalue formulation in mind we do not explicitly excite the resonators at the port interfaces and concentrate the modeling on the outgoing waves. The electric field strength can then be composed of individual mode contributions according to

$$\vec{E} = \sum_{\nu} A_{\nu} \left(\vec{E}_{t,\nu} + \vec{e}_z E_{z,\nu} \right) e^{-jk_{\nu}z} \quad (8)$$

where the full field is decomposed in terms of the transverse (t) and longitudinal (z) components. A local coordinate system is introduced such that $\vec{n} = \vec{e}_z$ represents the orientation of the outward normal vector of the relevant port plane. Following this approach the TEM, TE and TM modes in homogeneous waveguides can be described with only one formulation which is in addition even applicable for inhomogeneous port planes [3].

To evaluate the resulting boundary integral representation

$$\iint_{A_{\text{port}}} \frac{1}{\mu_r} (\vec{n} \times \text{curl } \vec{E}) \cdot \vec{\omega}_j^{3D} dA \quad (9)$$

the curl of the electric field can be rephrased analytically while special care has to be put in the analysis because of the fundamental differences in the handling of the transverse and longitudinal coordinates. The resulting expression

$$\vec{n} \times \text{curl } \vec{E} = \sum_{\nu} A_{\nu} \left(\text{grad } E_{z,\nu} + jk_{\nu} \vec{E}_{t,\nu} \right) \quad (10)$$

has already been evaluated in the port plane to simplify the notation. According to the orthogonality relation of the waveguide modes the missing scaling factors are specified according to the expression

$$A_{\nu} = \iint_{A_{\text{port}}} \varepsilon_r \vec{E} \cdot \vec{E}_{t,\nu}^* dA \quad (11)$$

which finally enables to set up the entire port boundary condition once the desired two-dimensional mode patterns are available for the specified port interfaces.

Port Description

Setting up a 3-D eigenvalue formulation where electromagnetic energy can dissipate through matched waveguides necessitates the calculation of the modal field pattern in the boundary plane together with the corresponding propagation constants. The desired modal data can be derived from a two-dimensional eigenvalue formulation once the evaluation frequency is fixed. In an iterative solution process the ultimate resonance frequency is then obtained by successive evaluation steps where the overall convergence rate depends on the coupling strength of the 2-D and 3-D fields. For practical applications regarding cavity simulations a few fixed-point iterations already lead to accurate results up to solver-precision.

The required field pattern $\vec{E}_{\nu} = \sum_i x_{i,\nu} \vec{\omega}_i^{2D}$ in the port plane can be calculated with the help of a 2-D eigenvalue formulation which is derived from the 3-D problem (3) with a necessary restriction to the port plane. Concentrating on the lossless case results in the notation

$$A^{2D} \vec{x}_{\nu} = \omega_{\nu}^2 \mu_0 \varepsilon_0 B^{2D} \vec{x}_{\nu} \quad (12)$$

with matrices A^{2D} and B^{2D} defined by the elements

$$A_{ij}^{2D} = \iint_{A_{\text{port}}} \frac{1}{\mu_r} \text{curl } \vec{\omega}_i^{2D} \cdot \text{curl } \vec{\omega}_j^{2D} d\Omega \quad (13a)$$

$$B_{ij}^{2D} = \iint_{A_{\text{port}}} \varepsilon_r \vec{\omega}_i^{2D} \cdot \vec{\omega}_j^{2D} d\Omega \quad (13b)$$

where the important propagation constants k_{ν} are hidden in the longitudinal dependence of the basis functions. Explicitly expanding the separated variables and simultaneously applying a partitioning of the weighting coefficients

according to the transverse and longitudinal components results in a block-oriented quadratic eigenvalue problem which can be also stated using the two equations

$$A_{11}^{2D} \vec{x}_t - jk_z B_{12}^{2D} \vec{x}_z + k_z^2 B_{11}^{2D} \vec{x}_t = 0 \quad (14a)$$

$$B_{22}^{2D} \vec{x}_z + jk_z B_{21}^{2D} \vec{x}_t = 0 \quad (14b)$$

and allows to determine the propagation constants once the evaluation frequency is fixed. The necessary submatrices are defined according to the expressions

$$A_{11,ij}^{2D} = \iint_{A_{\text{port}}} \frac{1}{\mu_r} \text{curl}_t \vec{\omega}_{t,i}^{2D} \cdot \text{curl}_t \vec{\omega}_{t,j}^{2D} d\Omega + \omega_{\text{port}}^2 \mu_0 \varepsilon_0 \iint_{A_{\text{port}}} \varepsilon_r \vec{\omega}_{t,i}^{2D} \cdot \vec{\omega}_{t,j}^{2D} d\Omega \quad (15a)$$

$$B_{11,ij}^{2D} = \iint_{A_{\text{port}}} \frac{1}{\mu_r} \vec{\omega}_{t,i}^{2D} \cdot \vec{\omega}_{t,j}^{2D} d\Omega \quad (15b)$$

$$B_{12,ij}^{2D} = \iint_{A_{\text{port}}} \frac{1}{\mu_r} \text{grad}_t \omega_{z,i}^{2D} \cdot \vec{\omega}_{t,j}^{2D} d\Omega \quad (15c)$$

$$B_{21,ij}^{2D} = \iint_{A_{\text{port}}} \frac{1}{\mu_r} \vec{\omega}_{t,i}^{2D} \cdot \text{grad}_t \omega_{z,j}^{2D} d\Omega \quad (15d)$$

$$B_{22,ij}^{2D} = \iint_{A_{\text{port}}} \frac{1}{\mu_r} \text{grad}_t \omega_{z,i}^{2D} \cdot \text{grad}_t \omega_{z,j}^{2D} d\Omega + \omega_{\text{port}}^2 \mu_0 \varepsilon_0 \iint_{A_{\text{port}}} \varepsilon_r \omega_{z,i}^{2D} \omega_{z,j}^{2D} d\Omega \quad (15e)$$

and have to be evaluated with the help of the 2-D basis functions in the specified port planes. The unfavorable quadratic formulation can be rephrased into the classical generalized eigenvalue problem

$$\begin{pmatrix} A_{11} & 0 \\ 0 & 0 \end{pmatrix} \begin{pmatrix} \vec{y}_t \\ \vec{y}_z \end{pmatrix} = -k_z^2 \begin{pmatrix} B_{11} & B_{12} \\ B_{21} & B_{22} \end{pmatrix} \begin{pmatrix} \vec{y}_t \\ \vec{y}_z \end{pmatrix} \quad (16)$$

using the substitutions $\vec{y}_t = k_z \vec{x}_t$ and $\vec{y}_z = -j \vec{x}_z$ [4]. The last equation in (16) is responsible for the source-free condition of the port modes although the derived formulation originates from Maxwell's curl equations only. The formulation is of particular interest because all eigenvalues and eigenvectors can be calculated using real-valued arithmetic even for the evanescent fields.

Once the 2-D eigenvalue problem (16) is solved for the lowest eigenvalues the extracted eigensolutions have to be incorporated into the originally stated 3-D formulation using the boundary representation (9). Because of the tangential nature of the vector expression $\vec{n} \times \text{curl} \vec{E}$ the essential equation can also be written in the form

$$\iint_{A_{\text{port}}} \frac{1}{\mu_r} (\vec{n} \times \text{curl} \vec{E}) \cdot \vec{\omega}_j^{2D} dA \quad (17)$$

where the 3-D basis functions have been interchanged with the corresponding 2-D variants without any approximation. Consequently, if the port-mode calculation has been performed on a 2-D subset of the 3-D discretization the specified integration does not have to be completed again but

can be copied instead from the 2-D calculations, where they have been carried out anyhow. This favorable feature is readily available if the applied 2-D basis functions are originating from the 3-D counterparts by projection on the specified port plane. All necessary basis functions automatically meet this fundamental requirement if the same construction scheme is used to set up the initially unknown vector functions from the known scalar counterparts.

Supplementary to the propagation constants the knowledge of the cut-off frequencies of the considered modes is advantageous to characterize the wave propagation. The necessary values do not have to be calculated from scratch but can be extracted from (16) with the help of a Rayleigh quotient simply by setting k_z to zero.

Splitting the submatrix in (15a) according to the definition $A_{11}^{2D} = A'_{11} - \omega_{\text{port}}^2 \mu_0 \varepsilon_0 A''_{11}$ into the specified parts A'_{11} and A''_{11} finally enables a simple incorporation of the boundary contribution (17) into the original eigenvalue formulation (3). Special care has been put in the conversions to demonstrate the symmetry of the resulting matrix block so that the entire formulation retains the favorable property.

IMPLEMENTATION

Based on the presented eigenvalue formulation a reliable computer program to enable high precision cavity simulations has been set up. The inherently high computational demands welcomes a parallel implementation utilizing distributed memory machines. The geometrical modeling of the structures is performed with the CST Studio Suite[®] [5]. A flexible tetrahedral mesh is used to perform the underlying FEM calculations. The electric field strength is described with the help of Nédélec-type basis functions up to the second order which are formulated on curved elements to retain the high approximation order even for non-flat material interfaces.

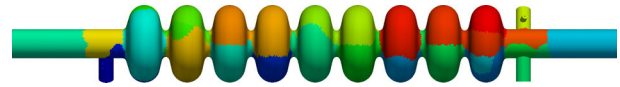


Figure 1: Partitioning of the computational domain among 32 processes. A unique color is assigned to each of the extracted sub domains to model e.g. a TESLA 9-cell cavity.

Because of the immanent coupling of excited modes to any kind of carefully designed loads the applied computer program explicitly has to enable a suitable handling of local loss mechanisms. The underlying algebraic eigenvalue solver naturally has to cope with a complex formulation which is not straightforwardly applicable to available solver packages. A robust realization of a Jacobi-Davidson-type eigenvalue solver has been implemented to extract the complex-valued eigenvectors and corresponding eigenvalues for the large 3-D problem while the 2-D port modes are determined as a comparable small problem with the help of standard LAPACK routines [6].

APPLICATION

The available algorithms have been applied to the computational model of a TESLA 1.3 GHz accelerating cavity to determine the complex resonance frequency of various configurations next to the corresponding field distributions for all modes e.g. in the first monopole passband and in the mixed first and second dipole passband [7]. The computational model consists of the nine-cell cavity, the fundamental input coupler as well as the up- and downstream higher-order modes couplers. Port boundary conditions are placed at the coaxial lines of the three couplers as well as on the two beam tubes.

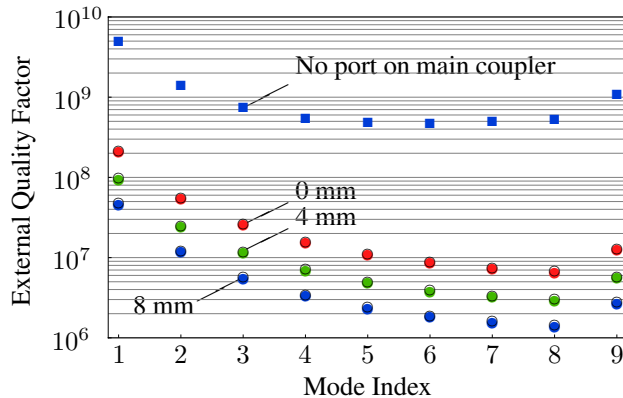


Figure 2: Quality factors for the monopole modes for various penetration depth of the main input coupler. The colored data points are obtained on a mesh using 1.3 million tetrahedrons (8.1 million complex DOF) while the black circles are included for comparison reasons and correspond to 283 thousand tetrahedrons (1.7 million complex DOF).

The implemented formulation can cover a wide range of dynamical systems reaching from strongly coupled configurations to nearly isolated resonators. A distinct feature of the complex formulation is given by the possibility to simultaneously determine the real part as well as the imaginary part of the angular resonance frequency. While the real part immediately characterizes the oscillation the imaginary part is used to describe the damping. Instead of directly specifying the damping coefficient the widespread quality factor $Q = \omega_{\text{real}} / (2\omega_{\text{imag}})$ is preferably used instead. Because the coupling to the external devices is the only loss mechanism considered in this work the quality factor is specified by the external quality factor only. In Figs. 2 and 3 selected simulation results are summarized to demonstrate a proper handling of the notoriously difficult large-scale numerical problem.

CONCLUSION

A robust FEM implementation of a dissipative eigenvalue formulation has been set up which enables to simulate lossy structures based on complex-valued variables without the necessity to precalculate real-valued systems in a preprocessing step. The available parallel computer program utilizes hierarchical Nédélec-type basis functions

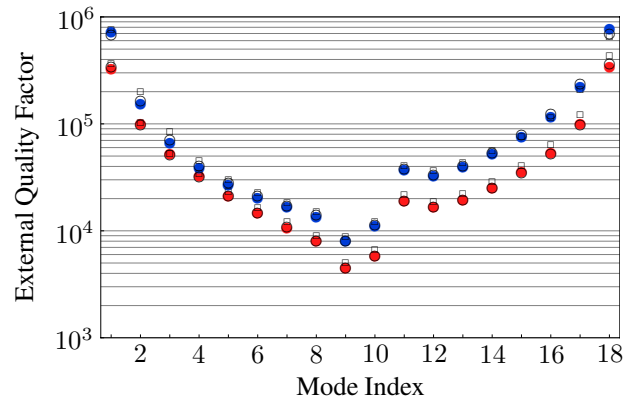


Figure 3: Quality factors for the 36 modes in the 1st and 2nd dipole band considering both polarizations. The calculations are performed on meshes with 0.354, 0.991 and 2.090 million tetrahedrons indicated by squared, circled and colored data points which translates to 2.1, 6.1 and 12.9 million complex degrees of freedom (DOF).

up to the second order on curved tetrahedral elements and can handle besides losses in bulk materials in particular an impedance boundary condition and a port mode representation for arbitrary number of ports. The practical applicability of the combined 2-D and 3-D formulation to real-life problems has been successfully demonstrated with the precise electromagnetic modeling of a TESLA-type accelerating cavity where the influence of the attached coupling units has been incorporated consistently in the formulation.

ACKNOWLEDGMENT

The Authors thank Martin Dohlus from DESY Hamburg, Germany, as well as Wolfgang F. O. Müller from the Technische Universität Darmstadt, Germany, for many valuable discussions on the physical problem formulations and the support for using the high performance computer.

REFERENCES

- [1] P. P. Silvester, R. L. Ferrari, *Finite Elements for Electrical Engineers*, Cambridge University Press, 1996
- [2] P. Ingelström, “A New Set of H(curl)-Conforming Hierarchical Basis Functions for Tetrahedral Meshes”, *IEEE Trans. on Microwave Theory and Techniques*, 54(1): 106-114, 2006
- [3] L.-Q. Lee, Z. Li, C. Ng, K. Ko, “Omega3P: A Parallel Finite-Element Eigenmode Analysis Code for Accelerator Cavities”, SLAC-PUB-13529, February 2009
- [4] C. J. Reddy, M. D. Deshpande, C. R. Cockrell, F. B. Beck, “Finite Element Method for Eigenvalue Problems in Electromagnetics”, NASA Technical Paper 3485, December 1994
- [5] CST AG - Computer Simulation Technology, CST Studio Suite 2012, <http://www.cst.com>
- [6] Intel Corporation, Intel Math Kernel Library 2011, LAPACK Math Functions, <http://www.intel.com>
- [7] M. Dohlus, V. Kaljuzhny, S. G. Wipf, “Higher Order Mode Absorption in TTF Modules in the Frequency Range of the 3rd Dipole Band”, TESLA Report 2002-05, 2002